

# Silver-Nanoparticle-Loaded Chitosan Lactate Films with Fair Antibacterial Properties

Rasika Tankhiwale, S. K. Bajpai

Polymer Research Laboratory, Department of Chemistry, Government Model Science College, Jabalpur 482001, India

Received 9 April 2009; accepted 18 July 2009

DOI 10.1002/app.31168

Published online 7 October 2009 in Wiley InterScience (www.interscience.wiley.com).

**ABSTRACT:** Food quality and safety are major concerns in the food industry. Antimicrobial packaging can be considered an emerging technology that could have a significant impact on life and food safety. Antimicrobial agents in food packaging can control the microbial population and target specific microorganisms to provide greater safety and higher quality products. In this work, a lactic acid grafted chitosan film was synthesized. Silver nanoparticles were loaded into the chitosan lactate (CL) film by equilibration in a silver nitrate solution, which was followed by citrate reduction. The presence of silver nanoparticles was con-

firmed with transmission electron microscopy, X-ray diffraction, Fourier transform infrared spectroscopy, and thermogravimetric analysis of the film. The silver-nanoparticle-loaded CL film was investigated for its antimicrobial properties against *Escherichia coli*. This newly developed material showed strong antibacterial properties and thus has potential for use as an antibacterial food-packaging material. © 2009 Wiley Periodicals, Inc. *J Appl Polym Sci* 115: 1894–1900, 2010

**Key words:** biodegradable; FT-IR; TEM; UV-vis spectroscopy

## INTRODUCTION

There is growing interest in edible coatings because of factors such as environmental concerns, new storage techniques, and the market development of underused agricultural commodities. Edible coatings and films prepared from polysaccharides, proteins, and lipids have a variety of advantages, such as biodegradability, edibility, biocompatibility, appearance, and barrier properties. To control food contamination and quality loss, edible coatings and biodegradable packaging have been recently introduced into food processing. Several applications have been reviewed, with a particular emphasis on the reduction of quality. The packaging can serve as a carrier for antimicrobial and antioxidant compounds to maintain a high concentration of preservatives on food surfaces. Their presence could prevent moisture loss during storage, reduce the rate of rancidity causing lipid oxidation and brown coloration, reduce the load of spoilage and pathogen microorganisms on the surfaces of foods, and restrict the loss of volatile flavors.<sup>1</sup> For edible films to be employed as food packaging materials, they should

satisfy the requirements of being durable, stress-resistant, flexible, pliable, and elastic. Thus, they should possess desirable tensile properties, being able to bear stresses exerted during various handling processes. These edible films are ecofriendly and user-friendly, and the raw materials are essentially derived from either replenishable agricultural feed stocks (cellulose, starch, and proteins) or marine food processing industry waste (chitin/chitosan).<sup>2</sup>

Chitosan is an ideal biopolymer for developing such antimicrobial films because of its nontoxicity,<sup>3</sup> biocompatibility,<sup>4</sup> biodegradability,<sup>5</sup> film-forming ability,<sup>6</sup> and inherent antimicrobial properties.<sup>7</sup> Moreover, the antimicrobial properties of chitosan can be enhanced by irradiation,<sup>8</sup> UV-radiation treatment, partial hydrolyzation,<sup>9</sup> chemical modifications,<sup>10</sup> synergistic enhancements with preservatives,<sup>11</sup> synergistic enhancements with antimicrobial agents,<sup>12</sup> or combination treatments with other hurdle technologies. One of the simplest and most economical ways of producing antimicrobial films is to incorporate antimicrobial substances into films.<sup>13</sup> Various organic acids that naturally occur in fruits and vegetables and possess general antimicrobial activity, such as acetic, lactic, malic, citric, sorbic, benzoic, and succinic acids, can be used for this purpose.<sup>14</sup> Furthermore, because chitosan needs to be dissolved in slightly acidic solutions, the production of antimicrobial films from chitosan with organic acids is straightforward.<sup>15</sup> Chitosan films formed with various organic acids such as acetic, formic, lactic, citric, propionic, and malic acids have various physicochemical properties.<sup>16,17</sup>

Correspondence to: R. Tankhiwale (rasika\_81@rediffmail.com).

Contract grant sponsor: Council of Scientific & Industrial Research [Human Resource Development Group (HRDG)], New Delhi; contract grant number: SRF (Ext) Project 8/31(0006)/2008-EMR-I.

Chitosan films exhibit selective permeability to gases<sup>18</sup> and possess a stronger texture. In general, edible films and coatings provide the potential to control the transport of moisture, oxygen, aromas, oils, and flavor compounds in food systems; this depends on the nature of the edible film-forming materials.<sup>19,20</sup> Manufacturing biopolymer-based films with adequate water barrier properties is a major challenge as many of the biopolymers are hydrophilic by nature.<sup>21</sup> Butler et al.<sup>18</sup> stated that their chitosan films were extremely good barriers to oxygen but had higher water vapor barrier properties because of their hydrophilic nature.

Because of disease transmission and cross-infections caused by microorganisms, the use of antimicrobial materials has increased in many application areas, such as protective clothing for medical and chemical work, other health-related products,<sup>22,23</sup> and antibacterial packaging materials that can improve product quality and keep products free from microbial adhesion.<sup>24</sup> Such antimicrobial packaging materials may be produced by the introduction of silver, gold, or copper nanoparticles into polymer films. In particular, silver has been recognized for its broad-spectrum antimicrobial activities.<sup>25,26</sup> Silver inactivates bacteria by interacting with the thiol groups of bacterial proteins and enzymes.<sup>27</sup> It has been proposed that silver ions ( $\text{Ag}^+$ ), released from silver nanoparticles ( $\text{Ag}^0$ ), interact with phosphorous moieties in DNA, resulting in the inactivation of DNA replication. In fact, silver nanoparticles are highly germicidal, quite harmless to humans, and absolutely nontoxic. It has been reported that even the highest concentration of nanosilver causes no side effects.<sup>28</sup> The antibacterial and antiviral actions of silver, silver ions, and silver compounds have been thoroughly investigated.<sup>29–32</sup> Silver nanoparticles have opened a new era in the fight against diseases such as methicillin-resistant *Staphylococcus aureus*, cystic fibrosis, and acquired immune deficiency syndrome and in the treatment of wounds (see <http://www.oaresearch.co.uk/pressrelease.pdf>). In a recent work by Wen et al.,<sup>33</sup> human fibroblasts were grown in various concentrations of silver nanoparticles during the period of observation. The results of their study demonstrated the nontoxicity of the interaction of nanometer-scale silver particles and the membrane surface. Although synthetic polymeric films are frequently used as packaging materials, their nondegradability has been a matter of great concern for environmentalists, and so attempts have been made to develop materials that can undergo degradation and are ecofriendly. In this connection, we synthesized a membrane as an antibacterial packaging material by grafting lactic acid onto chitosan; this was followed by the loading of silver nanoparticles with our recently developed approach.<sup>26</sup>

## EXPERIMENTAL

### Materials

Chitin (molecular weight = 400,000) was purchased from Hi Media Chemicals (Mumbai, India), and its deacetylation was carried out with 50% NaOH (w/v) at 90°C in an  $\text{N}_2$  atmosphere for 2 h. The final chitosan flakes were washed until the flakes were completely neutral and then were dried at 50°C in an electric oven (Temstar, India). Lactic acid, sodium hydroxide, silver nitrate ( $\text{AgNO}_3$ ), and trisodium citrate were obtained from E. Merck (Mumbai, India). A nutrient broth and nutrient agar were obtained from Hi Media Chemicals. Standard cultures of the organisms were provided by the Department of Biotechnology of Government Model Science College (Jabalpur, India). Double-distilled water was used throughout the investigations.

### Preparation of the plain chitosan lactate (CL) films

Chitosan flakes were dissolved in a 2 wt % lactic acid solution in an electric oven at 70°C for 1 h. The dissolved content was filtered, and the pale yellow solution was then poured into a uniform layer of 1-mm thickness onto a polypropylene plate. The optimum conditions for casting were 60°C and 2.5 h in a dry oven at the ambient relative humidity. When the lactic acid was completely evaporated, the glass plates were exposed to cold air. The glass plates were then dipped in 10 mL of a 1M NaOH solution to remove the chitosan membrane (CL membrane) from the glass plates. The membrane was then washed with distilled water to neutrality and then dried in a dust-free chamber.

### Loading of the silver nanoparticles into the CL films

The silver nanoparticles were loaded into the CL films with a novel approach developed in our laboratory.<sup>26</sup> Each CL film was put into a solution of  $\text{AgNO}_3$  [15 mg of  $\text{AgNO}_3$  in 40 mL of distilled water) for 12 h; it then was taken out and put into a trisodium citrate solution (20 mg dissolved in 25 mL of distilled water) for the next 12 h to reduce  $\text{Ag}^+$  ions into silver nanoparticles. The silver-nanoparticle-loaded film thus obtained was allowed to dry at the ambient temperature.

### Characterization of the silver-nanoparticle-loaded CL films

Transmission electron microscopy (TEM) measurements were performed with a JEOL JEM-2000 operating at 200 kV. The Fourier transform infrared (FTIR) spectra of the films were recorded on a

Shimadzu (Japan) 8400 S FTIR spectrophotometer. X-ray diffraction (XRD) analysis was performed with a Rigaku (Tokyo, Japan) diffractometer running at 40 kV and 40 mA. The thermal history of the plain CL film and silver-nanoparticle-loaded CL film was evaluated on a DuPont 2100 thermogravimetric analysis (TGA) instrument (USA) at a heating rate of 10°C/min.

### Microbial experimentation

The antibacterial activity of plain and silver-nanoparticle-loaded films was tested qualitatively and quantitatively with spread plates.<sup>34</sup> In all these methods, *Escherichia coli* was taken as a model bacterium. For qualitative measurements of the microbial activity, the films (plain CL and silver-nanoparticle-loaded CL) were cut to make a circle 7.4 cm in diameter, and the antimicrobial activity was tested with a modified agar diffusion assay (a disc test). The plates were examined for possible clear zones after incubation at 37°C for 2 days. The presence of any clear zone that formed on the surface of the film was recorded as an indication of inhibition against the microbial species.

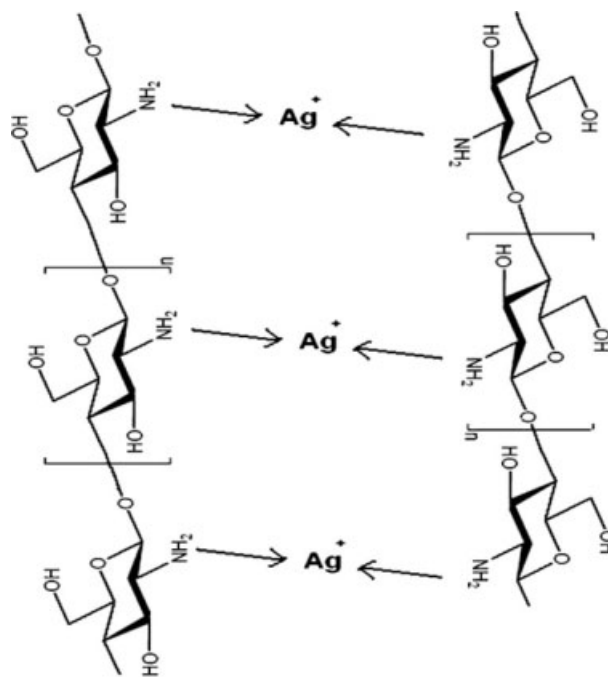
To examine the bacterial growth or killing kinetics of silver-nanoparticle-loaded CL films, approximately  $10^8$  cfu of *E. coli* cells were grown in 10 mL of a nutrient broth supplemented with the discs of the plain CL and silver-nanoparticle-loaded CL films for 24 h. The killing rate and bacterial concentrations were determined by their optical density values from time to time.

## RESULTS AND DISCUSSION

### Fabrication of the CL films

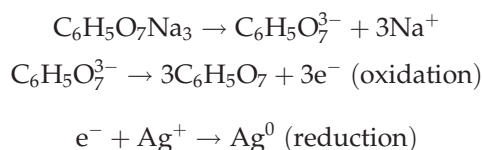
Chitosan is a chelating polymer with excellent binding capacities for a number of metal ions because of the parent amino ( $-\text{NH}_2$ ) and hydroxyl ( $-\text{OH}$ ) groups in its structure. Thus, one of the most important properties of chitosan is its ability to chelate heavy-metal ions. With the nitrogen electrons, the amino groups on chitosan serve as ligands or binding sites for metal ions, forming metal complexes. This chelating action of chitosan with silver ions can be represented as shown in Scheme 1.

Likewise, in the case of the preparation of chitosan-silver nanoparticles, the two coordination sites of silver are occupied by electron pairs of the two  $-\text{NH}_2$  groups of two different chitosan chains. Because chitosan is a semirigid polymer, the two  $-\text{NH}_2$  groups coordinated with silver ions are unlikely to be in the same chitosan chain because of steric hindrance. When a silver-ion-coordinated film is placed in a sodium citrate solution, silver ions are reduced to  $\text{Ag}^0$  and later yield nanoparticles.



**Scheme 1** Scheme showing the chelation of silver ions to chitosan chains.

The almost uniform presence of  $-\text{NH}_2$  groups within the chitosan film thus helps in obtaining a homogeneous distribution of silver nanoparticles. Therefore, crosslinked three-dimensional networks also serve as stabilizers for silver nanoparticles and prevent them from aggregating. The reduction process can be represented as follows:



### Characterization of the plain CL and silver-nanoparticle-loaded films

#### FTIR analysis

Figure 1(A,B) presents IR spectra of the plain CL film and the silver-nanoparticle-loaded CL film, respectively. The peak at  $3620\text{--}3590\text{ cm}^{-1}$  can be attributed to different vibrations: hydrogen-bonded OH stretching at  $3430\text{ cm}^{-1}$ ,  $\text{NH}_2$  asymmetric stretching at  $3502\text{ cm}^{-1}$ , and NH stretching in inter-chain  $\text{NH}\cdots\text{OC}$  bonding at  $3393\text{ cm}^{-1}$ .<sup>35</sup> The absorption of CH stretching of methyl or methylene groups is at  $2935\text{ cm}^{-1}$ . The absorption of  $\text{C}=\text{O}$  stretching is at  $1687\text{ cm}^{-1}$  (amide I band), and the amide II band is at  $1535\text{ cm}^{-1}$  (N-H in-plane deformation coupled with C-N stretching); amide III (C-N stretching coupled with N-H in-plane deformation) is found at  $1168\text{ cm}^{-1}$ . The peak observed in the range

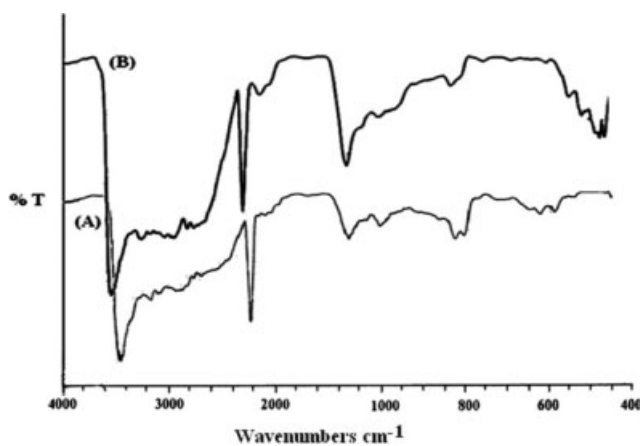


**Figure 1** FTIR spectra of (A) the plain CL film and (B) the silver-nanoparticle-loaded CL film.

of 800–600  $\text{cm}^{-1}$  results from out-of-plane N–H wagging.<sup>36</sup>

In the silver-nanoparticle-loaded CL film [Fig. 1(B)], the stretching vibrations at 3620–3590  $\text{cm}^{-1}$  are slightly shifted to 3614–3600  $\text{cm}^{-1}$ . Similarly, the amide II band at 1535  $\text{cm}^{-1}$  in the plain CL film is absent in the silver-nanoparticle-loaded CL film. This clearly indicates that silver binds to the functional groups of chitosan. Peak shifting occurs

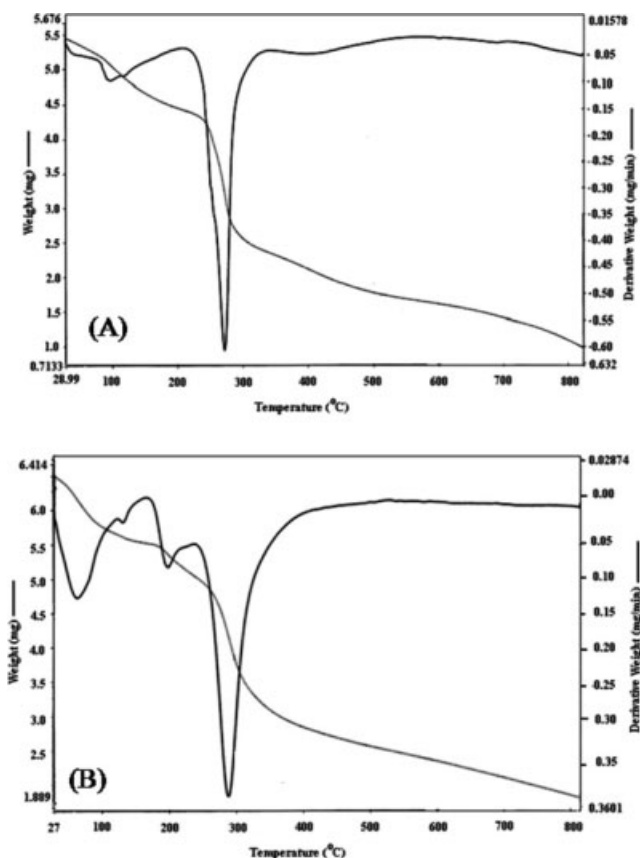


**Figure 2** Thermograms of (A) the plain CL film and (B) the silver-nanoparticle-loaded CL film.

**TABLE I**  
Initial Decomposition Temperature ( $T_{id}$ ), Final Decomposition Temperature ( $T_{fd}$ ), and Temperature of the Maximum Rate of Weight Loss ( $T_{max}$ )

| $T_{id}$ ( $^{\circ}\text{C}$ ) | $T_{fd}$ ( $^{\circ}\text{C}$ ) | $T_{max}$ ( $^{\circ}\text{C}$ ) |
|---------------------------------|---------------------------------|----------------------------------|
| 100                             | 300                             | 250                              |

because of the coordination between the heavy-metal atom (silver in this case) and electron-rich groups (oxygen/nitrogen). This causes an increase in the bond length, ultimately leading to a shift in the frequency. The C–N stretching vibration is found at 1168  $\text{cm}^{-1}$  for the plain CL film [Fig. 1(A)] and for the silver-nanoparticle-loaded CL [Fig. 1(B)]. Thus, the FTIR spectrum supports the presence of silver nanoparticles in the CL film.

### TGA

TGA of the plain CL and silver-nanoparticle-loaded films is shown in Figure 2(A,B), respectively. The initial weight loss, observed in both films, can be attributed to the loss of moisture present within the film. Later, an appreciable weight loss occurs between 100 and 200 $^{\circ}\text{C}$ , and the plain chitosan film suffers greater weight loss in comparison with the silver-loaded film. The main decomposition occurs from 250 to 300 $^{\circ}\text{C}$ . This should be due to the degradation of polysaccharide chains and dehydration of deacetylated units of chitosan. Total decomposition occurs at 800 $^{\circ}\text{C}$ . At the stage of total decomposition (800 $^{\circ}\text{C}$ ), the percentage mass of the chitosan/nano-silver film is  $50 \pm 0.5$  wt %, whereas that of the plain chitosan film is  $40 \pm 0.8$  wt %. This is clearly shown in Figure 2. Therefore, it may be claimed that the enhanced thermal stability of the chitosan/nano-silver film is an indication of the presence of silver nanoparticles in the film (Table I).

XRD, ultraviolet–visible (UV–vis) spectroscopy, and TEM analyses

XRD studies were performed on the silver-nanoparticle-loaded CL film. The peaks can be clearly seen in Figure 3. A broad diffraction peak at 22 $^{\circ}$

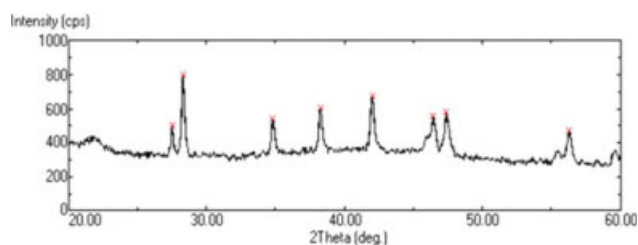


**Figure 3** XRD analysis of the silver-nanoparticle-loaded CL film. [Color figure can be viewed in the online issue, which is available at [www.interscience.wiley.com](http://www.interscience.wiley.com).]

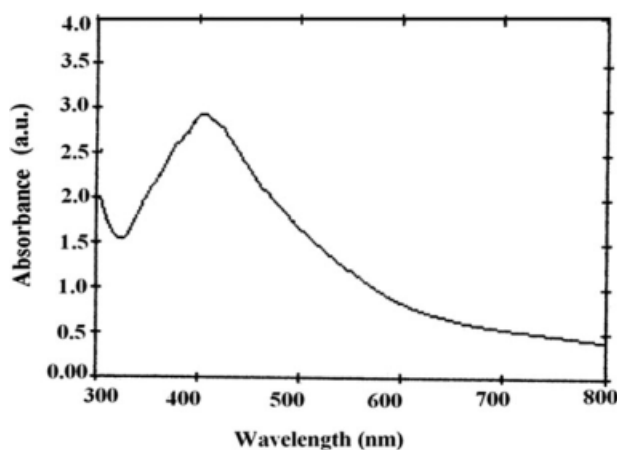


**Figure 4** UV-vis spectrum of the silver-nanoparticle-loaded CL film.

corresponds to the crystalline region of the chitosan.<sup>37</sup> Moreover, some strong peaks also appear at 28, 38, and 44° and indicate the presence of silver ions on the fabric surface;<sup>38</sup> they can be attributed to incomplete reduction. Finally, two strong peaks at 42.02 and 38.38° represent the (200) and (111) Bragg reflections of face-centered cubic structures of silver nanoparticles.<sup>39</sup> In this way, the XRD pattern confirms the formation of silver-nanoparticle-loaded chitosan attached to the cotton fabric. Finally, the grain size was evaluated with the well-known Scherrer equation:

$$D = \frac{K\lambda}{(b - b_0) \cos \theta}$$

where  $\theta$  is the angle of diffraction. A Cauchy peak type is assumed. Here  $D$  is the crystal size,  $\lambda$  is the

X-ray wavelength,  $b$  is the width of the peak (full width at half-maximum),  $b_0$  is the instrumental peak broadening, and  $K$  is the Scherrer constant (0.89). The crystal sizes for the (111) and (200) peaks were found to be 86 and 87 nm, thus indicating the formation of silver nanoparticles of almost uniform size.

Furthermore, to confirm the formation of silver nanoparticles in the film, we carried out UV-vis absorption studies. In Figure 4, a strong characteristic absorption peak around 408 nm can be noted for the silver nanoparticles in the film, and this is due to the surface plasmon resonance effect.

TEM images of the nanosilver-loaded CL film are depicted in Figure 5(A,B). The size distribution studies were made by the examination of the sizes of 50 particles in the TEM images. About 52% of the particles had an average diameter of approximately 166 nm, and 30% of the particles had an average diameter of approximately 133 nm. It may also be noted that the diameter of the formed nanoparticles was in the range of 75–250 nm [see Fig. 5(B)].

#### Antimicrobial activities of the silver-nanoparticle-loaded CL films

Silver nanoparticles demonstrate excellent antimicrobial activity alone<sup>40,41</sup> or within a polymer/hydrogel matrix.<sup>42,43</sup> Thus, they act as an excellent antibiofouling agent. Similarly, Yu et al.<sup>42</sup> prepared silver-embedded poly(L-lactic acid) membranes, and these were tested for their antibacterial activity against methicillin-resistant *S. aureus*. These membrane showed effective and long-term antibacterial activity. Besides these, silver-nanoparticle-loaded natural films and membranes are also being prepared now and are being tested for their antibacterial properties as natural polymers have many advantages over

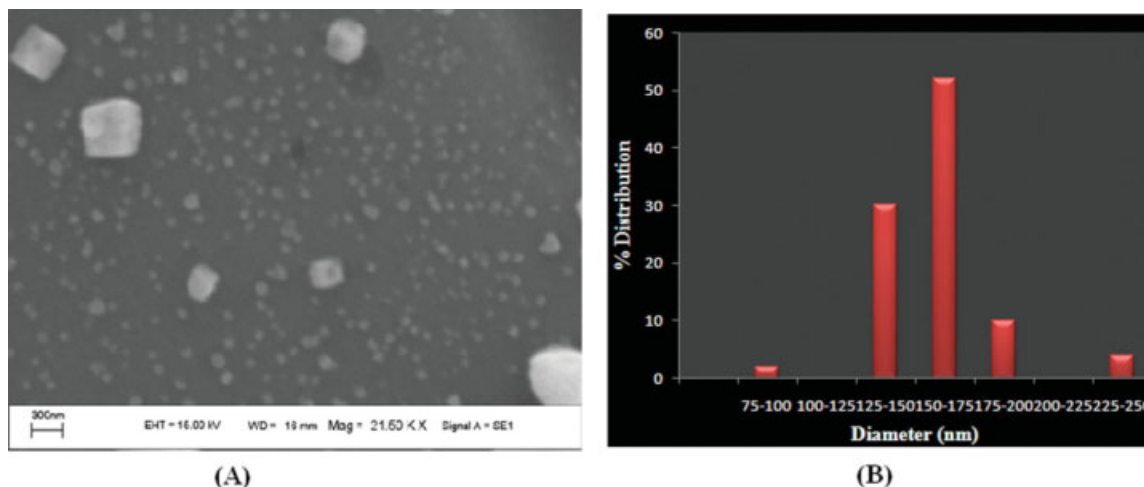


**Figure 5** (A) TEM image of the nanosilver-loaded CL film and (B) size distribution pattern of the particles in the film. [Color figure can be viewed in the online issue, which is available at [www.interscience.wiley.com](http://www.interscience.wiley.com).]

synthetic polymers. Here we investigated the biocidal action of the prepared nanosilver-loaded chitosan films; we considered *E. coli* as a model bacterium and observed its growth in the presence of the nanosilver-loaded chitosan films by the spread plate method.

For quantitative measurements, the spread plate method was used. The nutrient agar was spread onto a Petri plate over the whole chitosan film, and an *E. coli* culture was spread onto it. A marked difference was observed in the plates containing the plain chitosan films [Fig. 6(A)] and the silver-nanoparticle-loaded chitosan films [Fig. 6(B)]. It is quite clear that the growth of bacterial colonies was almost nil in the plate supplemented with a silver-loaded chitosan film, and this confirms the strong inhibitory action of nanosilver.

The growth rate or killing kinetics of the bacterium *E. coli* was determined in a nutrient broth for a period of 6 h, and the results were determined by optical density measurements. The results are clear in Figure 7. The optical density of the nutrient broth with plain chitosan discs was high in comparison with that of the nutrient broth with silver-nanoparticle-loaded chitosan discs. This clearly depicts that with time, the growth of *E. coli* cells was reduced in the nutrient broth containing silver-nanoparticle-loaded chitosan discs because of the antimicrobial activity.

## CONCLUSIONS

On the basis of this study, we can conclude that a novel and easy method has been discovered for preparing silver-nanoparticle-loaded CL films, characterizing them, and studying their antibacterial properties. The films exhibit excellent antimicrobial activity against *E. coli* and can be used as antibacterial packaging materials to prevent bacterial infections of foodstuff. This approach can be easily used

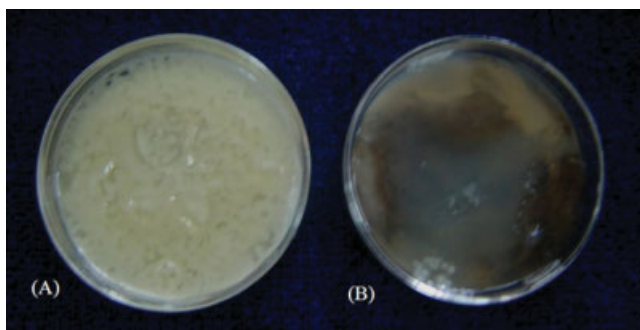


**Figure 6** Bacterial colonies on Petri plates: (A) plain and (B) silver-nanoparticle-loaded CL films. [Color figure can be viewed in the online issue, which is available at [www.interscience.wiley.com](http://www.interscience.wiley.com).]

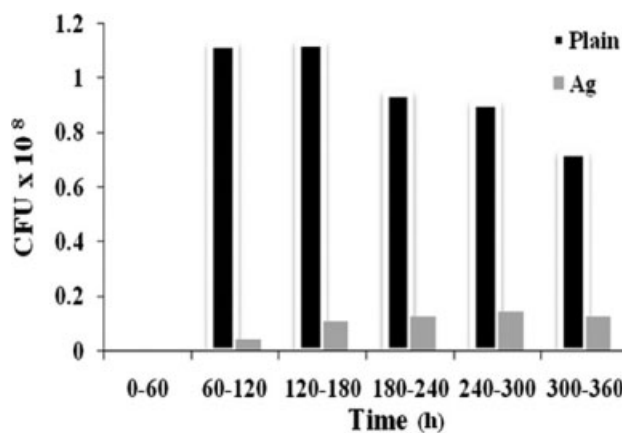


**Figure 7** Bar diagram showing the growth rates of *E. coli* in the presence of plain CL discs (black bars) and silver-nanoparticle-loaded CL discs (gray bars).

in the large-scale production of silver-nanoparticle-loaded chitosan films.

The authors thank O. P. Sharma, head of the Department of Chemistry, Government Model Science College, for providing facilities.

## References

- Pérez-Pérez, C.; Regalado-González, C.; Rodríguez-Rodríguez, C. A.; Barbosa-Rodríguez, J. R.; Villaseñor-Ortega, F. *Adv Agric Food Biotechnol* 2006, 661, 37.
- Srinivasa, P. C.; Tharanathan, R. N. *Food Rev Int* 2007, 23, 53.
- Hirano, S.; Itakura, C.; Seino, H.; Akiyama, Y.; Nonaka, I.; Kanbara, N.; Kanakami, T.; Arai, K.; Kinumaki, T. *J Agric Food Chem* 1990, 38, 1214.
- Muzzarelli, R. A. A. *Biomaterials* 1993, 20, 7.
- Shigemasa, Y.; Saito, K.; Sashiwa, H.; Saimoto, H. *Int J Biol Macromol* 1994, 16, 43.
- Averbach, B. L. In *Proceedings of the First International Conference on Chitin/Chitosan*; Muzzarelli, R. A. A.; Pariser, E. R., Eds.; Massachusetts Institute of Technology: Cambridge, MA, 1978; p 199.
- Sudarshan, N. R.; Hoover, D. G.; Knorr, D. *Food Biotechnol* 1992, 6, 257.
- Matsuhashi, S.; Kume, T. *J Sci Food Agric* 1997, 73, 237.
- Davydova, V. N.; Yermak, I. M.; Gorbach, V. I.; Krasikova, I. N.; Solov'eva, T. F. *Biochemistry* 2000, 65, 1082.
- Nishimura, K.; Nishimura, S.; Nishi, N.; Saiki, I.; Tokura, S.; Azuma, I. *Vaccine* 1984, 2, 93.
- Roller, S.; Sagoo, S.; Board, R.; O'Mahony, T.; Caplice, E.; Fitzgerald, G.; Fogden, M.; Owen, M.; Fletcher, H. *Meat Sci* 2002, 62, 165.
- Lee, C. H.; An, D. S.; Park, H. F.; Lee, D. S. *Packaging Technol Sci* 2003, 16, 99.
- Weng, Y. M.; Hotchkiss, J. H. *Packaging Technol Sci* 1993, 6, 123.
- Beuchat, L. R. *Surface Decontamination of Fruits and Vegetables Eaten Raw: A Review*. Food safety issues. World Health Organization: Geneva, 1998.
- Begin, A.; Calsteren, M. R. V. *Int J Biol Macromol* 1999, 26, 63.
- Park, H. J.; Jung, S. T.; Song, J. J.; Kang, S. G.; Vergano, P. J.; Testin, R. F. *Chitin Chitosan Res* 1999, 5, 19.
- Park, S. Y.; Marsh, K. S.; Rhim, J. W. *J Food Sci* 2002, 67, 194.
- Butler, B. L.; Vergano, P. J.; Testin, R. F.; Bunn, J. M.; Wiles, J. L. *J Food Sci* 1996, 61, 952.

19. Krochta, J. M. In *The Wiley Encyclopedia of Packaging Technology*; Brody, A. L.; March, K. S., Eds.; Wiley: New York, 1997.
20. Krochta, J. M.; De Mulder-Johnston, C. *Food Technol* 1997, 51, 61.
21. Webber, C. J. *Biobased Packaging Materials for the Food Industry: Status and Perspectives*. <http://www.mli.kvl.dk/foodchem/special/biopack> (accessed Jan 2005).
22. Margaret, I. P.; Sau, L. L.; Vincent, K. M. P.; Lung, I.; Bud, A. *J Med Microbiol* 2006, 55, 59.
23. Duran, N.; Marcato, P. D.; De Souza, G. I. H.; Alves, O. L.; Esposito, E. *J Biomed Nanotechnol* 2007, 3, 203.
24. Park, S. I.; Zhao, Y. *J Agric Food Chem* 2004, 52, 1933.
25. Galeano, B.; Korff, E.; Nicholson, W. L. *Appl Environ Microbiol* 2003, 69, 4329.
26. Tankhiwale, R.; Bajpai, S. K. *Colloids Surf B* 2009, 69, 164.
27. Lok, C. N.; Ho, C. M.; Chen, R.; He, Q. Y.; Yu, W. Y.; Sun, H.; Tam, P. K.; Chiu, J. F.; Che, C. M. *J Proteome Res* 2006, 5, 916.
28. Becker, O.; Robert, M. D.; Spardaro, A.; Joseph, J. *Bone Joint Surg A* 1978, 60, 871.
29. Sondi, I.; Salopek-Sondi, B. *J Colloid Interface Sci* 2004, 275, 177.
30. Pal, S.; Tak, Y. K.; Song, J. M. *Appl Environ Microbiol* 2007, 73, 1712.
31. Duran, N.; Marcato, P. D.; De Souza, G. I. H.; Alves, O. L.; Esposito, E. *J Nanotechnol* 2007, 3, 1.
32. Baker, C.; Pradhan, A.; Pakstis, L.; Pochan, D. J.; Shah, S. I. *J Nanosci Nanotechnol* 2005, 5, 244.
33. Wen, H.-C.; Lin, Y.-N.; Jian, S.-R.; Tseng, S.-C.; Weng, M.-X.; Liu, Y.-L.; Lee, P.-T.; Chen, P.-Y.; Hsu, R.-Q.; Wu, W.-F.; Chou, C.-P. *J Phys Conf Ser* 2007, 61, 445.
34. Thomas, V.; Shreedhar, B.; Yallapu, M. M.; Bajpai, S. K. *J Biomater Sci*, to appear.
35. Roeges, N. P. G. *A Guide to the Complete Interpretation of Infrared Spectra of Organic Structures*; Wiley: Chichester, England, 1994.
36. Silverstein, R. M.; Basseler, C. G.; Morrill, T. C. *Spectrometric Identification of Organic Compounds*, 5th ed.; Wiley: New York, 1991.
37. Masahisa, W.; Yukie, S. *J Polym Sci Part B: Polym Phys* 2001, 39, 168.
38. Kim, J. J. *Ind Eng Chem* 2007, 13, 718.
39. Yu, D.; Lin, W.; Lin, C.; Chang, L.; Yang, M. *Mater Chem Phys* 2007, 101, 93.
40. Shrivastava, S.; Bera, T.; Roy, A.; Singh, G.; Ramachandrarao, P.; Dash, D. *Nanotechnology* 2007, 18, 225103.
41. Sarkar, S.; Jana, A. D.; Samanta, S. K.; Mostafa, G. *Polyhedron* 2007, 26, 4419.
42. Yu, H.; Xu, X.; Chen, X.; Lu, T.; Zhang, P.; Jing, X. *J Appl Polym Sci* 2007, 103, 125.
43. Thomas, V.; Namdeo, M.; Yallapu, M. M.; Bajpai, S. K.; Bajpai, M. *J Macromol Sci Pure Appl Chem* 2008, 45, 107.